

# Measurements of single top-quark production with the ATLAS detector

W. H. Bell<sup>1</sup> on behalf of the ATLAS Collaboration

<sup>1</sup>Université de Genève, Section de Physique, 24 rue Ernest Ansermet, CH-1211 Genève 4

DOI: will be assigned

These proceedings summarise the single top-quark production cross-section results obtained with the ATLAS [1] detector at a centre-of-mass energy of 7 TeV. Cross-section results for the  $t$ ,  $Wt$  and  $s$ -channels are presented. These results are interpreted in terms of the CKM matrix element  $|V_{tb}|$  assuming  $|V_{tb}| \gg |V_{ts}|$  and  $|V_{td}|$ . Searches for flavour changing neutral-currents and right-handed  $W'$  in single top-quark events are also presented.

## 1 Introduction

Top-quark production in proton-proton collisions at the LHC [2] is dominated by top anti-top production processes. In contrast to the dominant production via flavour-conserving strong interactions, single top quarks are produced through the electroweak interaction. In the Standard Model (SM) three processes are responsible for single top-quark production: the exchange of a virtual  $W$ -boson in the  $t$  and  $s$  channels, and the associate production of a top quark and a real  $W$ -boson ( $Wt$ ).

Experimental measurements of the single top-quark production cross-section directly probe the  $W$ - $t$ - $b$  vertex, constraining possible sources of beyond the SM physics processes [3]. Cross-section measurements set constraints on the absolute value of  $V_{tb}$ , without an assumption on the number of quark generations. The same results can alternatively be used to constrain the  $b$ -quark parton density function (PDF) using the  $t$ -channel measurements. Within the SM, production of a single top-quark via flavour changing neutral currents (FCNC) is forbidden at the tree-level and suppressed at higher orders [4]. However, beyond the standard model theories, which include exotic quarks [5], new scalars [6], supersymmetry [7] and technicolour [8] predict higher FCNC rates.

## 2 Event selection

Data were selected using a high transverse momentum ( $p_T$ ) inclusive single lepton trigger. Electrons were then required to have cluster  $E_T$  greater than 25 GeV and an absolute pseudorapidity ( $|\eta|$ ) less than 2.47. Electron clusters within the barrel-endcap transition region  $1.37 < |\eta| < 1.52$  were excluded. Muons candidates were required to be within  $p_T > 25$  GeV and  $|\eta| < 2.5$ . Tight isolation requirements around the lepton candidate were made using the inner detector tracker and calorimeter, to reduce the QCD-multijet background contribution.



24 Jets were reconstructed using the anti- $k_t$  algorithm [9] and a radius parameter of 0.4. A tag-  
 25 ging algorithm based on the combination of secondary vertex and combined lifetime information  
 26 was used to tag jets from b-quark decays. The missing transverse momentum ( $E_T^{\text{miss}}$ ) was then  
 27 calculated from the reconstructed objects and unclustered calorimeter cells.

28 The event sample for the  $t$ -channel analysis [10] was defined by requiring exactly two or  
 29 three jets  $p_T > 25$  GeV and  $|\eta| < 4.5$ . Exactly one jet  $p_T > 25$  GeV and  $|\eta| < 2.5$  was required  
 30 to be b-tagged, with an efficiency of 57% and a light jet rejection factor of 520 (reciprocal of  
 31 light jet tagging efficiency). Events with more than one selected lepton were rejected. The  
 32 QCD-multijet background was reduced by requiring  $E_T^{\text{miss}} > 25$  GeV and the sum of the  $E_T^{\text{miss}}$   
 33 and transverse W mass  $m_T(W)$ <sup>1</sup> to be greater than 60 GeV. Events were selected for the  
 34 FCNC [11] and right-handed  $W'$  [12] searches using the same lepton, b-tagging, jet  $p_T$ ,  $E_T^{\text{miss}}$   
 35 and  $E_T^{\text{miss}} + m_T(W)$  requirements. For both searches, jets were required to be within  $|\eta| < 2.5$ .  
 36 In the case of the FCNC analysis, events with exactly one b-jets were selected, whereas the  $W'$   
 37 analysis required two jets and exactly one b-tag. The  $s$ -channel analysis [13] used a b-tagging  
 38 efficiency of 50% with a corresponding light jet rejection rate of 270. Exactly two jets ( $|\eta| < 2.5$ )  
 39 and one or two b-tagged jets  $|\eta| < 2.5$  were required.

40 Dilepton events were selected for the  $Wt$  analysis [14] by requiring exactly two selected lep-  
 41 tons with opposite charge. The backgrounds from Z boson processes were reduced by rejecting  
 42 events with a dilepton mass  $81 < m_{ll} < 101$  GeV and by requiring an azimuthal separation  
 43  $\Delta\phi(l_1, E_T^{\text{miss}}) + \Delta\phi(l_2, E_T^{\text{miss}}) > 2.5$ . The QCD-multijet background was reduced by requiring  
 44  $E_T^{\text{miss}} > 50$  GeV.

### 45 3 Analyses and results

46 The  $t$ -channel analysis was performed using multivariate and cut-based signal discrimina-  
 47 tion techniques. The dominant systematic uncertainties were found to be the initial and  
 48 final state radiation (14%) and the b-tagging efficiency (13%). In comparison, the statisti-  
 49 cal uncertainty was found to be 5%. The  $t$ -channel cross-section was determined to be  
 50  $\sigma_t = 83 \pm 4(\text{stat.}) \pm_{-19}^{+20}(\text{syst.})$  pb from the simultaneous measurement in the two and three  
 51 jet channels. A value of  $|V_{tb}|^2$  was extracted by assuming  $|V_{tb}| \gg |V_{td}|, |V_{ts}|$  and that the  
 52  $W$ - $t$ - $b$  interaction is a SM-like left-handed weak coupling. The cross-section measurement from  
 53 the neural network analysis was divided by the SM expectation to determine  $|V_{tb}|^2$ . Using  
 54 the constraint  $0 < |V_{tb}| < 1$ ,  $|V_{tb}|$  was found to be greater than 0.75 at the 95% confidence  
 55 level (CL). The separation between signal and background contributions for the output of the  
 56 neural network is shown in Fig. 1(a). The results of the multivariate and cut based analyses  
 57 are summarised in Fig. 1(b), and are found to be consistent with SM predictions.

58 The  $Wt$  analysis was performed using an integrated luminosity of  $0.70 \text{ fb}^{-1}$ . The dominant  
 59 systematic uncertainties were found to be the jet energy scale (35%), jet reconstruction efficiency  
 60 (33%), jet energy resolution (32%) and the top anti-top background (24%). The statistical  
 61 uncertainty was found to be 37%. The 95% CL observed (expected) cross-section limit was  
 62 found to be  $\sigma(pp \rightarrow Wt + X) < 39(41)$  pb.

63 The  $s$ -channel analysis was carried out for an integrated luminosity of  $0.70 \text{ fb}^{-1}$ . The  
 64 dominant uncertainties were found to be statistical (100%), MC generator modelling (60%) and

---

<sup>1</sup> $m_T(W)$  is defined as  $\sqrt{2p_T^l p_T^\nu (1 - \cos(\phi^l - \phi^\nu))}$ , where  $l$  and  $\nu$  refer to the lepton and neutrino terms respectively. In the event selection the neutrino terms were replaced with the  $E_T^{\text{miss}}$  and its azimuthal angle.

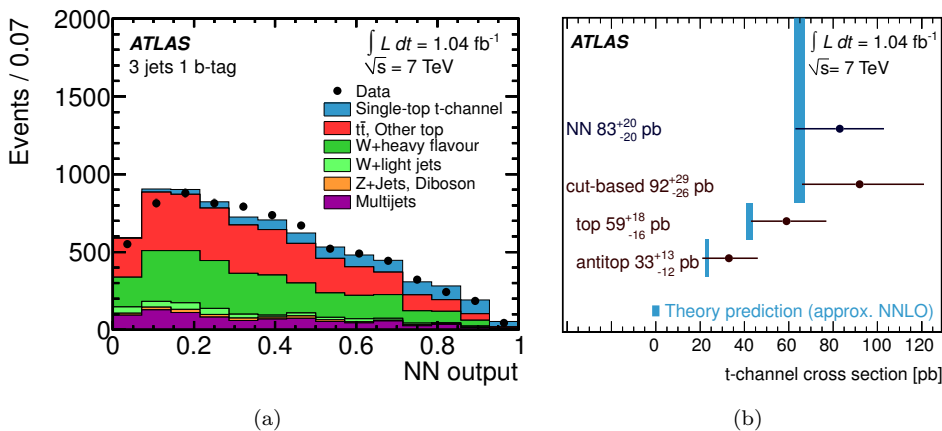


Figure 1: (a) Neural network output distribution in the 3-jet b-tagged sample [10]. All component distributions are normalised to the result of the maximum-likelihood fit. (b) Summary of the ATLAS single top-quark t-channel cross-section results [15]. Theoretical predictions obtained from N. Kidonakis, Phys. Rev. D 83 (2011) 091503 (approximate NNLO) are shown by the vertical bands.

luminosity (50%). A cross-section limit was extracted using a likelihood function, including the statistical uncertainties, nuisance parameters for the systematic uncertainties, and a Gaussian constraint on the luminosity. The observed (expected) cross-section limit was found to be  $\sigma(pp \rightarrow Wt + X) < 26.5(20.5)$  pb.

The FCNC search was carried out in the framework of the  $t$ -channel analysis using an integrated luminosity of  $2.05 \text{ fb}^{-1}$ . The largest systematic uncertainties were the jet  $p_T$  and  $\eta$ -dependent scale factors (23–45%). A binned likelihood method was applied to the neural network output distributions, including the systematic and statistical uncertainties. Since no significant rate of FCNC is observed, an upper limit on the production cross-section was determined to be 3.9 pb at 95% CL. The resulting limit on the branching fractions  $t \rightarrow ug$  and  $t \rightarrow cg$  is shown in Fig. 2(a).

A right-handed  $W'$  search was performed within the framework of the  $s$ -channel analysis, and an integrated luminosity of  $1.04 \text{ fb}^{-1}$ . Following the event selection, the  $m_{tb}$  mass shown in Fig 2(b) was used to discriminate between signal and background events. The dominant systematic uncertainties were found to be the jet energy scale and the b-tagging scale factors (8–20%). No statistically significant excess was observed in the selected data. Upper limits on the cross-section times branching ratio were found to be 6.1–1.0pb at the 95% CL for  $W'$  masses of 0.5–2.0 TeV. The limits were translated into a lower bound on the allowed right-handed  $W'$  mass of greater than 1.13 TeV at the 95% CL.

## 4 Conclusion

The ATLAS collaboration has performed a complete set of single top-quark analyses, using data collected from  $pp$  collisions at a centre-of-mass energy of 7 TeV. The measurements and limits on each of the components of the single-top production cross-section have been performed and

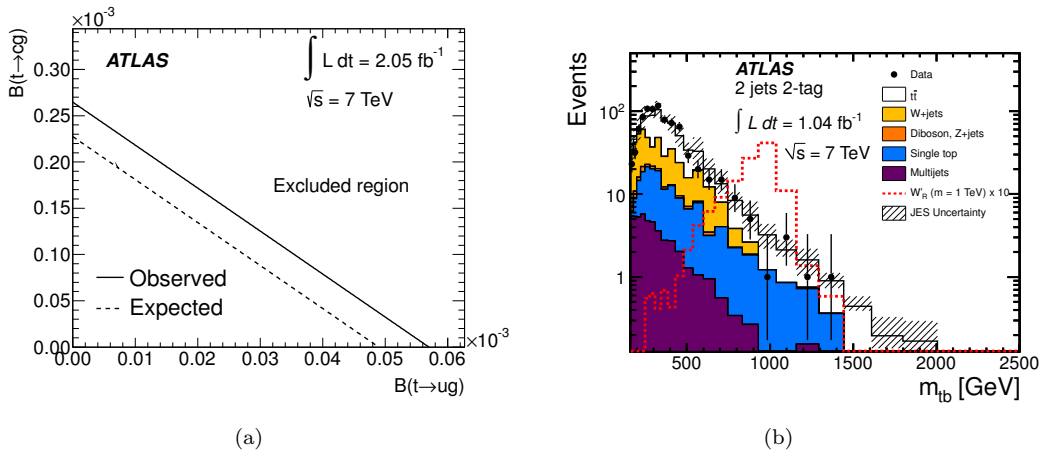


Figure 2: (a) Upper limit on the branching fractions  $t \rightarrow ug$  and  $t \rightarrow cg$  [11]. (b) The distribution of  $m_{tb}$  for double-tagged two-jet events compared to Standard Model expectations [12]. The expected  $W'$  signal was normalised to the theoretical cross-section and then scaled by a factor of 10.

88 found to be in agreement with standard model predictions. Limits on the production of single  
 89 top quarks via FCNC and right-handed  $W'$  have been established.

## 90 References

- 91 [1] The ATLAS Collaboration. JINST **3** (2008) S08003.  
 92 [2] L. Evans, (ed.) and P. Bryant, (ed.). JINST **3** (2008) S08001.  
 93 [3] T. M. Tait and C.-P. Yuan. Phys.Rev. **D63** (2000) 014018, arXiv:hep-ph/0007298 [hep-ph].  
 94 [4] S. Glashow, J. Iliopoulos, and L. Maiani. Phys.Rev. **D2** (1970) 1285–1292.  
 95 [5] J. Aguilar-Saavedra. Phys.Rev. **D67** (2003) 035003, arXiv:hep-ph/0210112 [hep-ph].  
 96 [6] S. Bejar, J. Guasch, and J. Sola. Nucl.Phys. **B600** (2001) 21–38, arXiv:hep-ph/0011091 [hep-ph].  
 97 [7] J. M. Yang, B.-L. Young, and X. Zhang. Phys.Rev. **D58** (1998) 055001, arXiv:hep-ph/9705341 [hep-ph].  
 98 [8] G.-r. Lu, F.-r. Yin, X.-l. Wang, and L.-d. Wan. Phys.Rev. **D68** (2003) 015002, arXiv:hep-ph/0303122  
 99 [hep-ph].  
 100 [9] M. Cacciari, G. P. Salam, and G. Soyez. JHEP **0804** (2008) 063, arXiv:0802.1189[hep-ph].  
 101 [10] The ATLAS Collaboration. arXiv:1205.3130 [hep-ex].  
 102 [11] The ATLAS Collaboration. Phys.Lett. **B712** (2012) 351–369, arXiv:1203.0529 [hep-ex].  
 103 [12] The ATLAS Collaboration. arXiv:1205.1016 [hep-ex].  
 104 [13] The ATLAS Collaboration. ATLAS-CONF-2011-118.  
 105 [14] The ATLAS Collaboration. ATLAS-CONF-2011-104.  
 106 [15] “Measurement of the t-channel single top-quark production cross section in  $pp$  collisions at  $\sqrt{s} = 7$  TeV  
 107 with the ATLAS detector”.  
 108 <https://atlas.web.cern.ch/Atlas/GROUPS/PHYSICS/PAPERS/TOPQ-2011-14/>.